

Electronic structure of neutral and charged vacancies in GaAs

Hongqi Xu

Department of Theoretical Physics, University of Lund, Sölvegatan 14A, S-223 62 Lund, Sweden

U. Linddefelt

Corporate Research Division, Asea Brown Boveri A.B., S-721 78 Västerås, Sweden

(Received 31 July 1989; revised manuscript received 28 November 1989)

We have performed self-consistent tight-binding calculations on the neutral and charged states of the undistorted Ga and As vacancies in GaAs with the Lanczos-Haydock recursion method. For neutral states, defect potentials on the first- and second-nearest neighbors of a vacancy are obtained by a charge-neutrality condition, while for charged states these potentials are determined self-consistently. A discussion of the nature of both anion and cation vacancies in III-V compound semiconductors in terms of the bulk properties is given. The general characteristics of the electronic structure of the vacancies in GaAs are extracted from a detailed calculation and analysis in the case where a vacancy is neutral. In addition, we have calculated the electronic structure for the various charge states of the vacancies in GaAs. The predicted trends for the bound electron states in the gap are presented. Our results agree well with the self-consistent local-density-theory calculation for GaAs: V_{Ga}^0 and GaAs: V_{As}^0 of Bachelet *et al.* and with the recently published positron-annihilation-spectroscopy data for two charge-state transitions of the arsenic vacancy, $V_{\text{As}}^{2-} \rightarrow V_{\text{As}}^-$ and $V_{\text{As}}^- \rightarrow V_{\text{As}}^0$, by Corbel *et al.*

I. INTRODUCTION

In III-V semiconductor compounds, vacancies are important native defects which can exist in both sublattices. In principle, the defects introduce localized states into the fundamental gap and can be neutral or negatively and positively charged depending on the position of the Fermi level. Further, vacancies are mobile and can thus migrate in the material and be trapped by other native defects or impurities to form vacancy-related complexes.

Optical- and electrical-spectroscopy techniques have been extensively used to study various defects and their complexes in semiconductors.^{1,2} However, these techniques give signals which are difficult to analyze for vacancies and for their related complexes in GaAs,³ although the isolated Ga vacancy in GaP has been identified by Kennedy *et al.* through electron-paramagnetic-resonance (EPR) experiments.^{4,5} Recently, positron-annihilation spectroscopy, which has proved to be a powerful method to study vacancy-type defects, has been used to study vacancies in GaAs.^{3,6-8} Corbel *et al.*³ reported a systematic investigation of the positron annihilation in GaAs. They found two Fermi-level-controlled transitions. They proposed that the two transitions correspond to two charge-state transitions of the arsenic vacancy, $V_{\text{As}}^{2-} \rightarrow V_{\text{As}}^-$ and $V_{\text{As}}^- \rightarrow V_{\text{As}}^0$.

Theoretical calculations of the deep levels of various defects have been carried out with emphasis on the simplest isolated defects.¹ The Green's-function methods, mainly developed in the late 1970s and early 1980s,⁹⁻¹² are presently the most commonly used methods in the calculations of the electronic structure of localized defects in semiconductors. The calculations have supplied

some information to experimentalists for defect identifications.

In this paper, we report a systematic theoretical calculation of the electronic structure of ideal isolated vacancies in GaAs for the neutral and for the various charged states by the self-consistent tight-binding scheme. In Sec. II, we present the method of calculation. In Sec. III, we discuss the general nature of the vacancies in III-V compound semiconductors, and then present and analyze the results of our calculation. Comparisons with a calculation based on the local-density theory¹³ and with data from positron-annihilation spectroscopy experiments³ are also given in this section. Finally, in Sec. IV we summarize our findings and discussions.

II. METHOD OF CALCULATION

A. Tight-binding Hamiltonian for the perfect crystal

Our calculation is based on the tight-binding approximation in an sp^3 basis including both first- and second-nearest-neighbor interactions. The perfect-crystal Hamiltonian H_0 then takes the form

$$H_0 = \sum_{i,\sigma,\mathbf{R}} |i\sigma\mathbf{R}\rangle [E_0(\mathbf{R})]_i \langle i\sigma\mathbf{R}| + \sum_{\substack{i,j,\sigma \\ \mathbf{R},\mathbf{R}'}} [|i\sigma\mathbf{R}\rangle [V_0(\mathbf{R},\mathbf{R}')]_{ij} \langle j\sigma\mathbf{R}'| + \text{H.c.}], \quad (1)$$

where $i = s, p_x, p_y, \text{ or } p_z$ label the orbitals, σ is the spin (\uparrow or \downarrow), \mathbf{R} denotes atomic-site vectors, and H.c. stands for Hermitian conjugate. $[E_0(\mathbf{R})]_i$ is the diagonal element of H_0 in the basis $|i\sigma\mathbf{R}\rangle$ and the transfer-matrix

elements $[V_0(\mathbf{R}, \mathbf{R}')_{ij}]$ are nonzero only between the nearest- and the second-nearest-neighbor atoms, i.e., when $|\mathbf{R} - \mathbf{R}'| = \sqrt{3}a/4$ or $\sqrt{2}a/2$, where a is the cubic lattice constant. The state $|i\sigma\mathbf{R}\rangle$ is a localized orbital centered on the cation at \mathbf{L} or on the anion at $\mathbf{L} + \mathbf{d}$, where \mathbf{L} is the lattice vector in the fcc lattice and $\mathbf{d} = (1, 1, 1)a/4$ is the vector between nearest neighbors. Our choice of Hamiltonian is the sp^3 nearest- and second-nearest-neighbor tight-binding Hamiltonian of Strehlow *et al.*¹⁴ The advantage of this Hamiltonian is that besides its good fitting to the nonlocal empirical pseudopotential band structure of Chelikowsky and Cohen,¹⁵ the Hamiltonian gives the correct direction of charge transfer ($0.203e^-$ from cation to anion) for GaAs and relates the orbital diagonal energies to the orbital occupancies. Finally, we mention that in this calculation the host crystal has been approximated by a supercell containing 1331 pairs of Ga and As atoms and is subject to periodic boundary conditions.^{12,16} We then create a vacancy in the crystal by simply removing an atom from the supercell.

B. Defect potential and self-consistency

In the presence of vacancies, the Hamiltonian is altered from H_0 to H , where $H = H_0 + U$ and U is the defect potential due to the vacancy. In an sp^3 basis, H takes the same form as H_0 :

$$H = \sum_{i,\sigma,\mathbf{R}} |i\sigma\mathbf{R}\rangle E_i(\mathbf{R}) \langle i\sigma\mathbf{R}| + \sum_{\substack{i,j,\sigma, \\ \mathbf{R}, \mathbf{R}'}} [|i\sigma\mathbf{R}\rangle V_{ij}(\mathbf{R}, \mathbf{R}') \langle j\sigma\mathbf{R}'| + \text{H.c.}] . \quad (2)$$

We include in U the potential at the vacancy site as well as on the first and second shells of atoms around the vacancy and ignore lattice relaxation. For the vacancy site, the diagonal matrix elements of the defect potential can be taken as infinite in magnitude and the off-diagonal matrix elements as zero. This procedure is equivalent to cutting the bonds between the vacancy "atom" and the rest of the crystal. In a number of calculations,^{9,17-20} this simple approximation has been used to describe the vacancy potential without any other perturbation involved and the qualitative properties of the defect systems have been obtained. However, with this simple approximation alone, one usually obtains too small t_2 - a_1 level splitting,²¹ and furthermore one cannot treat charge-state-splitting effects of defect levels. To overcome these shortcomings, we also include in the defect potential U the following parts: (1) off-diagonal perturbation potential matrix elements between the atoms in the first shell around each vacancy, and (2) diagonal perturbation potential matrix elements for the atoms in the first and second shells around each vacancy. The former gives rise to larger t_2 - a_1 splitting in general, and the latter affects the occupation numbers for the orbitals.

The off-diagonal matrix elements are related to the two-center hopping integrals $(A, l; B, l'; m)_n$ in the forms given by Slater and Koster.²² These integrals $(A, l; B, l'; m)_n$ represent the interaction between an elec-

tron in the l th orbital on atom A with an electron in the l' th orbital on atom B through spherical potentials located on the two atoms, and $m = \sigma$ or π using conventional notation from molecular-orbital theory. Furthermore, $n = 1$ or 2 denotes the n th-nearest-neighbor distance. We further assume, following van der Rest and Pecheur,²¹ that for the orbitals l and l' these two-center hopping integrals $(A, l; B, l'; m)_n$ are given by the Wolfsberg-Helmholz formula,²³ which is written as

$$(A, l; B, l'; m)_n = \frac{1}{2} K_m (E_l + E_{l'}) [S(A, l; B, l')]_n , \quad (3)$$

where E_l and $E_{l'}$ are the diagonal eigenvalues of the l and l' orbitals, $[S(A, l; B, l')]_n$ is overlap integral between these two orbitals, and K_m is a constant. It has been shown²¹ that the assumption of an orthogonal basis made everywhere else in this paper is consistent with the appearance of an overlap integral in Eq. (3). For orbital l (or orbital l'), we use for the radial part the asymptotic form of the solution to the radial Schrödinger equation for the Coulomb potential $-e^2/r$:

$$R_l(r) = N r^{\gamma_l} e^{-\mu_l r} , \quad (4)$$

where N is a normalization constant and μ_l is related to the eigenvalue E_l by

$$\hbar^2 \mu_l^2 / (2m) = -E_l \quad (5)$$

and $\gamma_l = (e^2 m) / (\hbar^2 \mu_l) - 1$, which has been approximated by zero in our calculation, according to the discussion presented by Harrison.²⁴ The dependence of the matrix elements on the relative direction of the two interacting orbitals has been given explicitly in the classical paper by Slater and Koster.²² The overlap integrals $[S(A, l; B, l')]_n$ is then directly evaluated from these orbitals. With the Wolfsberg-Helmholz formula, we modify the two-center hopping integrals $(A, l; B, l'; m)_n$ for the imperfect solids from the bulk values $(A, l; B, l'; m)_{0n}$. For example, if we want to calculate a two-center hopping integral with respect to an As s orbital on site \mathbf{R}_1 and another As s orbital on site \mathbf{R}_2 , both atoms being adjacent to a Ga vacancy, we get (assuming K_m is a pure constant)

$$(As, s; As, s; m)_2 = (Ga, s; As, s; m)_{01} \times \frac{E_s(As) + E_s(As)}{E_s(Ga) + E_s(As)} \frac{[S(As, s; As, s)]_2}{[S(Ga, s; As, s)]_1} .$$

Once we know these two-center hopping integrals, we know the off-diagonal matrix elements of H and then the corresponding off-diagonal elements of the defect potential U .

For neutral vacancies, approximate self-consistency can be obtained by a local charge-neutrality condition.²⁵ The s -like and p -like orbital energies (E_s and E_p) on the atoms in the two nearest shells of a vacancy are given by

$$\begin{aligned} E_s^1 &= E_{0s}^1 + \Delta E^1 , \\ E_p^1 &= E_{0p}^1 + \Delta E^1 , \end{aligned} \quad (6a)$$

and

$$\begin{aligned} E_s^2 &= E_{0s}^2 + \Delta E^2, \\ E_p^2 &= E_{0p}^2 + \Delta E^2, \end{aligned} \quad (6b)$$

where E_{0s}^1 , E_{0p}^1 , E_{0s}^2 , and E_{0p}^2 are the bulk orbital energies, and ΔE^1 and ΔE^2 are energy shifts. Here, we specify the orbital energy on an atom in the first and second shells of a vacancy by using superscripts 1 and 2, respectively. ΔE^1 and ΔE^2 are adjusted in such a way that the total charge on the four first-nearest-neighbor atoms of a vacancy plus the charge on the removed (free) atom is equal to the total charge on the five corresponding atoms in the bulk crystal and that the total charge on the second-nearest-neighbor atoms of the vacancy is equal to the total charge on the corresponding atoms in the bulk crystal. In our calculation, we obtain $\Delta E^1=0.3622$ eV and $\Delta E^2=0.1624$ eV for the neutral Ga vacancy, and $\Delta E^1=0.0426$ eV and $\Delta E^2=0.0214$ eV for the neutral As vacancy.

For charged vacancies, the local charge-neutrality condition may not be valid. Instead, approximate self-consistency is achieved by using an empirical model of Coulomb effects in semiconductors developed by Sankey and Dow.²⁶ The model is expressed in terms of three different electron repulsion parameters U_{ss} , U_{pp} , and U_{sp} , together with two atomic bare ionization energies E_s^0 and E_p^0 , by the following formulas:

$$E_{s\sigma}(\{n_\alpha\}) = E_s^0 + \sum_{\sigma'} n_{s\sigma'} U_{ss} + \sum_{j,\sigma'} n_{p_j\sigma'} U_{sp} \quad (7a)$$

and

$$E_{p_j\sigma}(\{n_\alpha\}) = E_p^0 + \sum_{j,\sigma'} n_{p_j\sigma'} U_{pp} + \sum_{\sigma'} n_{s\sigma'} U_{sp}, \quad (7b)$$

where $j=x, y, \text{ or } z$, σ is the spin (\uparrow or \downarrow), the prime on the summation indicates that the self-interaction is excluded, and n_α is the occupation number for spin orbital α . Sankey and Dow determined a set of the five parameters E_s^0 , E_p^0 , U_{ss} , U_{pp} , and U_{sp} , using the requirement that Hartree-Fock s - and p -electron energies and the observed

ionization potentials of the free atoms be reproduced. They successfully applied their model to the various charge states of tetrahedral interstitial s - and p -bonded impurities in Si (Ref. 26) and also to the charge states of substitutional chalcogen impurities in Si.²⁷ In this paper, we are going to use their parameters to construct the defect potential for the charged vacancies. The method for calculating the spin-orbital occupation numbers n_α will be described in the next subsection.

For a given vacancy, we first calculate the diagonal matrix elements for the spin orbitals on the atoms on the first two nearest-neighbor shells of the vacancy from Eq. (7), when the vacancy is neutral. We then calculate, for an input defect potential U , the occupation numbers of these orbitals for a charged state of the vacancy and recalculate the diagonal matrix elements using these spin-orbital occupation numbers. The new diagonal matrix elements of the defect potential U are finally constructed from

$$\begin{aligned} U_\alpha &= \langle \alpha | (H^{\text{charged}} - H_0) | \alpha \rangle \\ &= \langle \alpha | (H^{\text{charged}} - H^{\text{neutral}}) | \alpha \rangle + \langle \alpha | (H^{\text{neutral}} - H_0) | \alpha \rangle \\ &= E_\alpha^{\text{charged}} - E_\alpha^{\text{neutral}} + \Delta E_\alpha^n, \end{aligned} \quad (8)$$

where $|\alpha\rangle$ stands for the spin orbitals $|i\sigma\mathbf{R}\rangle$ on the first two nearest neighbors of the vacancy, while $n=1$ or 2 has the same meaning as in Eq. (6). This procedure is repeated iteratively until self-consistency is obtained.

C. The recursion method

To obtain self-consistency, we must calculate the electronic occupancy n_α of the spin orbital α for the input defect potential U which, of course, is a function of $\{n_\alpha\}$. A very efficient method for accomplishing this is the recursion method.²⁸ In this method, the diagonal element of the Green's function $G_{\chi\chi}(E)$ for a given Hamiltonian H can be calculated in terms of the continued fraction,

$$G_{\chi\chi}(E) = \langle \chi | (E - H)^{-1} | \chi \rangle = \frac{1}{E - a_0 - \frac{b_1^2}{E - a_1 - \frac{b_2^2}{E - a_2 - \frac{b_3^2}{\ddots}}}}, \quad (9)$$

where $|\chi\rangle$ is a localized orbital which could be a symmetrized orbital or simply a simple atomic spin orbital $|i\sigma\mathbf{R}\rangle$ as in Eqs. (1) and (2). The coefficients a_n, b_n are generated, as we transform the given Hamiltonian H to a tridiagonal form, by the recursion relation

$$b_{n+1} |u_{n+1}\rangle = H |u_n\rangle - a_n |u_n\rangle - b_n |u_{n-1}\rangle, \quad (10)$$

where $\{|u_n\rangle\}$ is a new orthonormal basis set starting with the first element $|u_0\rangle$ set equal to $|\chi\rangle$. The physical quantities characterizing the system such as the local density of states (LDOS) $\rho_\chi(E)$ for the (starting) orbital

$|\chi\rangle$ and the electronic occupancy n_χ of the orbital are then obtained from the relations

$$\rho_\chi(E) = -\frac{1}{\pi} \lim_{\epsilon \rightarrow 0} \text{Im} G_{\chi\chi}(E + i\epsilon) \quad (11)$$

and

$$n_\chi = \int_{-\infty}^{E_f} \rho_\chi(E) dE. \quad (12)$$

In principle, the continued fraction is infinite in length for an infinite crystal, but in practice it is always truncat-

ed at some finite level and the effects of the remaining tail of the continued fraction are approximated by a terminator $t(E)$. A commonly used terminator is the square-root terminator^{29,30} which replaces the gap by a region of low density of states.

An alternative way to calculate the quantities ρ_χ and n_χ is with the quadrature approach developed by Nex.^{30,31} When the recursion in Eq. (10) is truncated at some finite level N , an approximate tridiagonal Hamiltonian H^N of dimension N is obtained:

$$H^N = \begin{pmatrix} a_0 & b_1 & 0 & 0 & 0 & 0 \\ b_1 & a_1 & b_2 & 0 & 0 & 0 \\ 0 & b_2 & a_2 & b_3 & 0 & 0 \\ 0 & 0 & b_3 & a_3 & b_4 & 0 \\ & & & \ddots & \ddots & \ddots \\ & & & & & a_{N-2} & b_{N-1} & 0 \\ & & & & & b_{N-1} & a_{N-1} & b_N \\ & & & & & 0 & b_N & a_N \end{pmatrix}. \quad (13)$$

The local density of states ρ_χ^N corresponding to H^N is given by

$$\begin{aligned} \rho_\chi^N(E) &= \sum_i^N |\langle E_i^N | \chi \rangle|^2 \delta(E - E_i^N) \\ &= \sum_i^N w_{\chi i}^N \delta(E - E_i^N), \end{aligned} \quad (14)$$

where E_i^N and $|E_i^N\rangle$ are eigenvalues and eigenstates of H^N , respectively, and $w_{\chi i}^N$ is called the weight of the eigenstate $|E_i^N\rangle$. The corresponding n_χ^N is

$$n_\chi^N = \int_{-\infty}^{E_f} \rho_\chi^N(E) dE = \sum_i^{\text{occ}} w_{\chi i}^N, \quad (15)$$

where the summation runs over occupied states only. The local density of states $\rho_\chi(E)$ for the starting orbital $|\chi\rangle$ and the electronic occupation number n_χ of the orbital $|\chi\rangle$ are limit values of $\rho_\chi^N(E)$ and n_χ^N with $N \rightarrow \infty$:

$$\rho_\chi(E) = \lim_{N \rightarrow \infty} \rho_\chi^N(E) \quad (16)$$

and

$$n_\chi = \lim_{N \rightarrow \infty} n_\chi^N. \quad (17)$$

In practice we seldom go beyond $N=150$.

The central quantity for the calculation of the local density of states and the electronic occupancy in the quadrature approach is evidently the weight $w_{\chi i}^N$. It has been shown by Nex³¹ that the weight $w_{\chi i}^N$ can be computed from the following equation:

$$w_{\chi i}^N = \frac{q_N(E_i^N)}{p'_{N+1}(E_i^N)}, \quad (18)$$

where $p_N(E_i^N)$ and $q_N(E_i^N)$ are two polynomials satisfying the three-term recurrence relations

$$p_{n+1}(E_i^N) = (E_i^N - a_n)p_n(E_i^N) - b_n^2 p_{n-1}(E_i^N), \quad (19a)$$

$$q_{n+1}(E_i^N) = (E_i^N - a_{n+1})q_n(E_i^N) - b_{n+1}^2 q_{n-1}(E_i^N), \quad (19b)$$

with the initial conditions $p_{-1}(E_i^N) = q_{-1}(E_i^N) = 0$, $p_0(E_i^N) = 1$, and $q_0(E_i^N) = b_0^2 = 1$.

Our experience has shown that for semiconductors it is convenient to use the terminator approach for estimating the density of states, whereas we find it better to use the quadrature approach for computing the electronic occupancy of spin orbitals if high accuracy is required. (It has been shown by experiment that the charge splittings of the energy levels for the vacancies in GaAs could be smaller than 0.1 eV in magnitude.³ Thus, the accuracy of the electronic occupancy of the spin orbitals should not be lower than of the order of 0.01 electron.) Because of this requirement and the fact that the energy levels in the gap are localized, we have used the Lanczos scheme^{32,33} to find the gap levels for various charge states and then the quadrature approach to calculate the electronic occu-

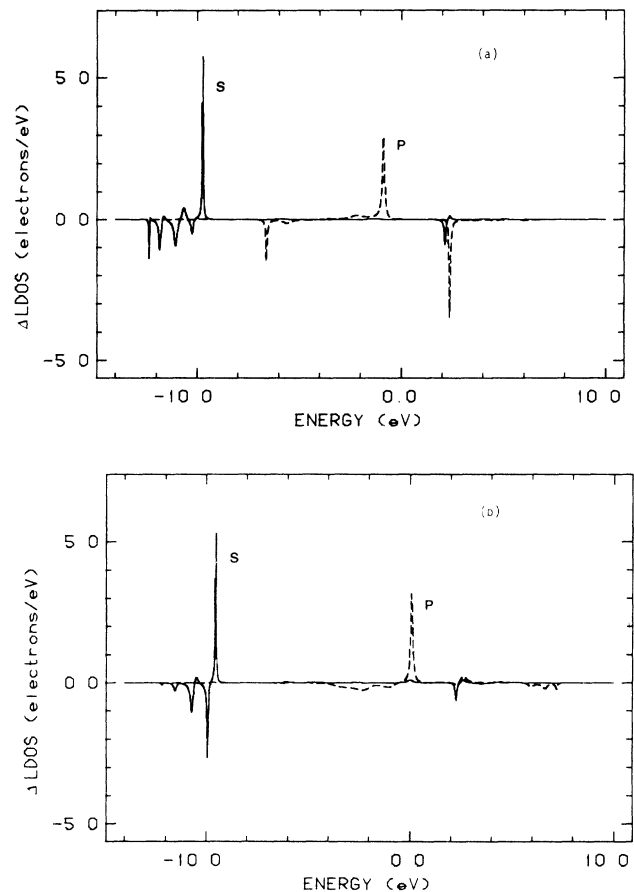


FIG. 1. Change in the local density of states (Δ LDOS) for the neutral undistorted Ga vacancy in GaAs using two a_1 and two t_2 symmetric orbitals constructed as linear combinations of neighboring s -like orbitals (denoted by s) and of neighboring p -like orbitals pointing towards the vacancy site (denoted by p). (a) Δ LDOS for a_1 symmetric orbitals, and (b) Δ LDOS for t_2 symmetric (x -like) orbitals. Units are electrons per eV. The spin degeneracy is excluded.

pation numbers of the spin orbitals on the atoms around the vacancy. When self-consistency is achieved, the localization of the gap levels can be directly evaluated from the calculated weights of the levels. The self-consistent local density of states for various symmetrized and unsymmetrized starting orbitals for the imperfect solid, as well as for the perfect crystal, is finally estimated by the square-root terminator approach.

III. RESULTS AND DISCUSSION

In this section, we present the results of our calculation for the neutral and charged vacancies in GaAs. The neutral vacancies are theoretically the most studied native defects in GaAs. The calculation with the local-density theory on the neutral vacancies performed by Bachelet *et al.*¹³ has given much information and physical insight into the electronic structure of the defects, and could be considered as the basic material to monitor the validity of any other more simple theory. Thus, it is worthwhile to show our results for the neutral vacancies and compare them with those of Bachelet *et al.* In addition, our results will supply some more intuitive information about the neutral vacancies. For the charged vacancies, we focus on the trends in their energy levels and the localizations of the wave functions corresponding to these levels. Comparisons of our results for the charged vacancies with experimental work and with some other theoretical calculations are presented. As the starting point of this section, we begin by discussing the general physical nature of the ideal vacancies in III-V zinc-blende-structure semiconductors, which will lead us to an intuitive interpretation of the calculated results.

A. Nature of the native vacancies

In a III-V zinc-blende-structure semiconductor, like GaAs, the anions are more electronegative than the cations. As a consequence, the creation of a cation vacancy is expected to produce a weaker perturbation than the creation of an anion vacancy. Since the perturbation due to a vacancy is repulsive, it can push levels from the valence band into the fundamental band gap. As it has been verified that an ideal vacancy in the homopolar semiconductor Si has a neutral defect level in the middle of the fundamental gap,¹⁰⁻¹² we may expect the cation

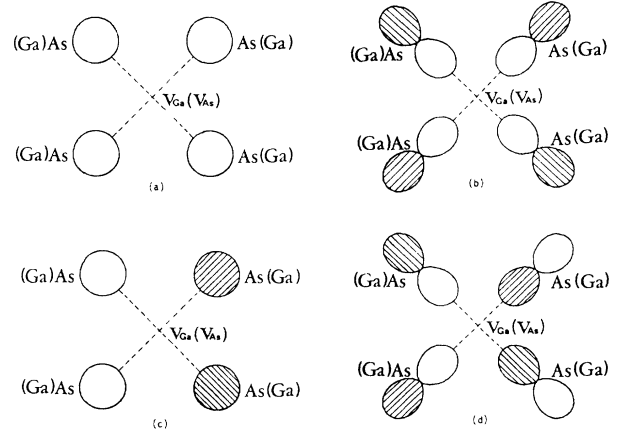


FIG. 2. Four inequivalent local symmetry orbitals constructed from the neighboring s orbitals of a vacancy and from the neighboring p orbitals pointing towards the vacancy site. (a) a_1 symmetric orbital $|\phi_s^{a_1}\rangle$ from the neighboring s orbitals, (b) a_1 symmetric orbital $|\phi_{p_{111}}^{a_1}\rangle$ from the neighboring p orbitals, (c) t_2 symmetric (x -like) orbital $|\phi_s^{t_2}\rangle$ from the neighboring s orbitals, and (d) t_2 -symmetric (x -like) orbital $|\phi_{p_{111}}^{t_2}\rangle$ from the neighboring p orbitals. The hatched regions indicate the negative part of the orbital.

vacancy to give rise to a defect level in the lower half of the fundamental gap and an anion vacancy to give a level in the upper half of the gap.

We will now begin a general discussion of the amount of s and p character in the gap state wave function for both cation and anion vacancies. In ascending order, the diagonal orbital energies of anions and cations in a III-V compound semiconductor are $E_s^a, E_s^c, E_p^a, E_p^c$, where the superscripts a and c denote anion and cation, respectively. For example, in the tight-binding Hamiltonian of Strehlow *et al.*,¹⁴ these energies for the GaAs crystal are $-17.312, -12.938, -8.939, \text{ and } -5.965$ eV in the above order. Since a pair of orbitals close in energy tend to interact more than if they are far apart in energy, we may conclude that for a cation the s orbital interacts more with the orbitals of the neighboring anions than its p orbital, while for an anion the p orbital interacts more with

TABLE I. Characteristic energy levels of the isolated neutral Ga and As vacancies in GaAs. The energies of the levels are measured relative to the top of the valence band. The width of the fundamental gap E_g is 1.51 eV, while the lower gap is in energies between 6.88 and 9.75 eV below the top of the valence band. The values of the two upper levels as calculated in Ref. 13, as well as the t_2 - a_1 splittings in both our calculation and the calculation in Ref. 13, are included for comparison. All energies are in eV.

	Ours					Ref. 13		
	Near lower gap		Near upper gap			Near upper gap		
	a_1	t_2	a_1	t_2	t_2 - a_1	a_1	t_2	t_2 - a_1
V_{Ga}^0	-9.65	-9.50	-0.88	0.168	1.05	-1.0	0.06	1.06
V_{As}^0	-6.86		-0.25	1.295	1.55	-0.8	1.08	1.88

the orbital of the neighboring cations than its s orbital. If we further consider the fact that an atom has one s orbital and three p orbitals, we conclude that for an anion in a III-V compound semiconductors its p -like orbitals contribute more to a bond than its s -like orbital. But for a cation, the situation is not so simple. In fact, although for a cation in a III-V compound semiconductor one p orbital contributes less to a bond than one s orbital, three p orbitals all together could contribute more to the bond than the single s orbital. Actually, if we keep in mind that a bond in a III-V compound semiconductor is formed by the interaction of the p orbitals of an anion with the orbitals of a cation and that both s and p orbitals of the cation are roughly equally close in energy to the p orbitals of the anion, it seems fully plausible that the bond is really due to the p character of the anion and the s and p characters of the cation. Nevertheless, for the cation one s orbital is always more important for the formation of the bond than one p orbital. We note that this feature of bonding in a III-V compound semiconductor is different from that in a group-IV covalent semiconductor, where the two identical sp^3 hybrid orbitals on the two identical atoms interact to form a bond. When we remove an atom from a III-V compound semiconductor to create a vacancy, the bonds around the vacancy site are broken and the remaining parts of these broken bonds for cation and anion vacancies are different. For the vacancy of a cation the broken bonds contain mainly the p character of anion atoms, whereas for the vacancy of an anion the broken bonds contain both the s and p characters of cation anions. As a consequence, we may expect that in a III-V compound semiconductor the gap level of a cation vacancy is essentially due to the p orbitals of the neighboring anions and that the gap level of an anion vacancy could be due to both the s and p orbitals of the neighboring cations.

B. Results for the neutral vacancies

We first present our results for the neutral Ga vacancy in GaAs. In Fig. 1, we display the change in the local density of states of the a_1 and t_2 symmetrical orbitals, each constructed from the four neighboring As s orbitals of the vacancy or from the neighboring As p orbitals pointing towards the vacancy. Looking at the changes in

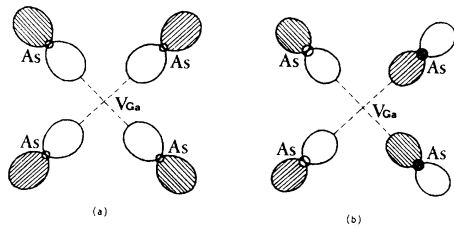


FIG. 3. Schematic representation of wave-function amplitudes for (a) the a_1 resonance at -0.88 eV and (b) the t_2 gap level at 0.17 eV for the neutral Ga vacancy in GaAs. The diameter of the s orbitals (circles) and the half-length of the p orbital (dumbbells) are scaled by their amplitudes. A hatched region in a wave function indicates a negative part of the wave function.

TABLE II. Weights for the characteristic energy levels of the neutral Ga vacancy, corresponding to the local symmetry orbitals constructed as linear combinations of the neighboring s and p orbitals, the latter pointing towards the vacancy site (see Fig. 2).

a_1			t_2		
level (eV)	Level weight $ \phi_s^{a_1}\rangle$	Level weight $ \phi_{p_{111}}^{a_1}\rangle$	level (eV)	Level weight $ \phi_s^{t_2}\rangle$	Level weight $ \phi_{p_{111}}^{t_2}\rangle$
-9.65	0.223	0.003	-9.50	0.468	0.003
-0.88	0.016	0.600	0.17	0.032	0.469

the local density of states in Fig. 1, we can see that for a_1 symmetry the ideal neutral Ga vacancy has a bound state at an energy close to the upper edge of the lowest s band and a strong resonance at 0.88 eV below the top of valence band. The a_1 bound state appears due to a loss of states in the s band, whereas the a_1 resonance appears largely because of the rearrangement of states within the valence band. For t_2 symmetry, the vacancy has two bound states, one in the lower gap due to the loss of states in the s band, and one in the fundamental gap due to the loss of the states in the valence band. The binding energy of the t_2 state in the fundamental gap is 0.17 eV and the energy of the lower bound state is at -9.50 eV, 0.25 eV above the upper edge of the lowest s band. These characteristic energy positions together with the (upper) t_2 - a_1 level splittings have been listed in Table I (upper half), where the results of the local-density theory of Bachelet *et al.*¹³ have also been included for comparison.

Figure 2 shows the four local symmetry orbitals which have been used as starting orbitals to calculate the local densities of states in Fig. 1. The calculated weights of the characteristic energy levels of the Ga vacancy for these orbitals are listed in Table II. As a first approximation, the wave functions of these energy levels can be approximated by linear combinations of these orbitals. The expansion coefficients can be determined from these weights by the method described in the Appendix. The proper linear combinations (partial wave functions) formed for the two a_1 levels and the two t_2 levels are listed in Table III. The amplitudes of the partial wave functions for the two upper levels are shown in Fig. 3, where the local electronic feature of these two levels can be clearly seen. The

TABLE III. Proper linear combinations (partial wave functions) formed from the local symmetry orbitals of Fig. 2 for the characteristic energy levels of the neutral Ga vacancy in GaAs. For the t_2 energy levels, we only list the partial wave functions for the x -like states.

Energy level	Symmetry	Partial wave function
-9.65	a_1	$0.47 \phi_s^{a_1}\rangle - 0.05 \phi_{p_{111}}^{a_1}\rangle$
-9.50	t_2	$0.68 \phi_s^{t_2}\rangle - 0.05 \phi_{p_{111}}^{t_2}\rangle$
-0.88	a_1	$0.13 \phi_s^{a_1}\rangle + 0.77 \phi_{p_{111}}^{a_1}\rangle$
0.17	t_2	$0.18 \phi_s^{t_2}\rangle + 0.68 \phi_{p_{111}}^{t_2}\rangle$

t_2 level at 0.17 eV above the lower edge of the fundamental gap and the a_1 resonance level at 0.88 eV below the edge appear mainly as the combinations of the p -like orbitals of the neighboring As atoms, whereas the t_2 level at 0.25 eV and the a_1 level at 0.10 eV (not shown) above the upper edge of the lowest s band appear mainly as the combinations of the s -like orbitals of the neighboring As atoms (see Table III and Fig. 3). For the t_2 level in the fundamental gap, this feature of the wave function is just what we expect (see Sec. III A). The same goes for the wave function for the a_1 resonance level. It is not difficult to understand the electronic features of the two lower levels at energies above the edge of the lowest s band. Both of these two states are pushed out by the vacancy repulsive potential from the s band. Although the band is essentially due to the s orbitals of the As atoms, there indeed exists a certain amount of the s and p character of the Ga atoms in the band. Nevertheless, since the removed Ga atom has brought its s and p orbitals from the crystal, the two levels could not have the s - and p -orbital characters of the removed atom. Their very localized features tell us that the two levels should be due to the s orbitals of the neighboring As atoms.

It is worthwhile to note that the broken antibonding orbitals in the conduction band also contribute to the t_2 gap level and the a_1 resonance at the top of the valence band. For instance, the p -like a_1 symmetric resonance at energy 0.88 eV below the top of the valence band [see Fig. 1(a)] has a contribution from both the antibonding orbitals in the conduction band and the bonding orbitals in the valence band. This is the reason for the two p -type negative peaks in Δ LDOS in Fig. 1(a).

We will now present our results for the neutral As vacancy in GaAs. We start with a description of the change in the local density of states (Fig. 4) for a_1 and t_2 symmetric starting orbitals. The starting orbitals are constructed for the As vacancy in the same way as for the Ga vacancy (Fig. 2). The only difference is that the atomic orbitals are provided by the Ga atoms in this case instead of by the As atoms in the previous situation. Two strong a_1 resonances appear at energies close to the lower and upper edges of the valence band. For the t_2 symmetry, only a localized bound state at 1.30 eV above the top of the valence band appears and no strong resonance is clearly found. Our calculated energy levels for these characteristic states and the t_2 - a_1 splitting between the two levels near the fundamental gap are also listed in

TABLE IV. Weights for the characteristic energy levels of the neutral As vacancy, corresponding to the local symmetry orbitals constructed as linear combinations of the neighboring s and p orbitals, the latter pointing towards the vacancy site (see Fig. 2).

a_1 level (eV)	Level weight		t_2 level (eV)	Level weight	
	$ \phi_s^{a_1}\rangle$	$ \phi_{p_{111}}^{a_1}\rangle$		$ \phi_s^{t_2}\rangle$	$ \phi_{p_{111}}^{t_2}\rangle$
-6.86	0.172	0.001	1.29	0.268	0.136
-0.25	0.065	0.357			

TABLE V. Proper linear combinations (partial wave functions) formed from the local symmetry orbitals of Fig. 2 for the characteristic energy levels of the neutral As vacancy in GaAs. For the t_2 gap level, we only list the partial wave functions for the x -like state.

Energy level	Symmetry	Partial wave function
-6.86	a_1	$0.41 \phi_s^{a_1}\rangle - 0.03 \phi_{p_{111}}^{a_1}\rangle$
-0.22	a_1	$0.25 \phi_s^{a_1}\rangle + 0.60 \phi_{p_{111}}^{a_1}\rangle$
1.29	t_2	$0.52 \phi_s^{t_2}\rangle + 0.37 \phi_{p_{111}}^{t_2}\rangle$

Table I (lower half) together with the results of Bachelet *et al.*¹³

In Table IV we list the calculated weights of the characteristic energy levels corresponding to the local symmetry orbitals displayed in Fig. 2 for the As vacancy

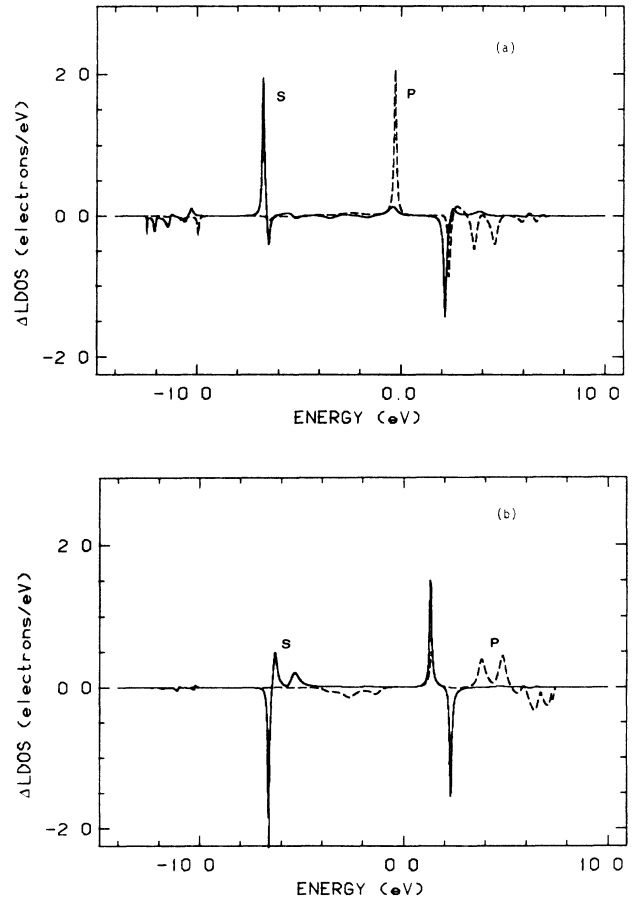


FIG. 4. Change in the local density of states (Δ LDOS) for the neutral undistorted As vacancy in GaAs using two a_1 and two t_2 symmetric orbitals constructed as linear combinations of neighboring s -like orbitals (denoted by s) and of neighboring p -like orbitals pointing towards the vacancy site (denoted by p). (a) Δ LDOS for a_1 symmetric orbitals, and (b) Δ LDOS for t_2 symmetric (x -like) orbitals. Units are electrons per eV. The spin degeneracy is excluded.

TABLE VI. Predicted a_1 and t_2 levels around the band gap and their t_2 - a_1 splittings due to the Ga vacancy in GaAs. The energies of the levels are measured relative to the valence-band edge. The column labeled t_2 level occupancy indicates electron occupation of the levels in the different charge states. The a_1 levels are always fully occupied.

Charge state	a_1 (eV)	t_2 (eV)	t_2 - a_1 (eV)	t_2 level occupancy
V_{Ga}^{3-}	-0.39	0.605	1.00	6
V_{Ga}^{2-}	-0.58	0.436	1.02	5
V_{Ga}^{1-}	-0.75	0.283	1.03	4
V_{Ga}^0	-0.88	0.168	1.05	3
V_{Ga}^{1+}	-0.96	0.100	1.06	2
V_{Ga}^{2+}	-1.01	0.068	1.08	1
V_{Ga}^{3+}	-1.03	0.051	1.08	0

in GaAs. From these weights we construct the local wave functions of these levels around the vacancy using the same procedure as we did in the case of the Ga vacancy. These local wave functions are listed in Table V. The amplitudes of the local wave functions for the two upper levels only are shown in Fig. 5, where the local electronic features of the two levels are schematically presented. In the region around the As vacancy, the a_1 resonance at an energy close to the lower gap appears as a combination of nearly pure s -like orbitals of the neighboring Ga atoms, whereas the a_1 resonance near the fundamental gap appears as a combination of mainly p -like orbitals of the neighboring Ga atoms. The t_2 level in the fundamental gap is very similar to the Si vacancy gap state, except that there is more atomic s character and less atomic p character in the broken bond than would be expected from a dangling sp^3 bond in Si. This feature of the wave function for the t_2 gap level fits very well with our earlier discussion in the previous subsection.

Our results for the ideal neutral Ga and As vacancies are in good agreement with the calculation by Bachelet *et al.*¹³ using the local-density theory. It could be pointed out that the t_2 gap levels and the upper a_1 levels which we found are higher in energy than the levels found by Bachelet *et al.*, but the local features of these

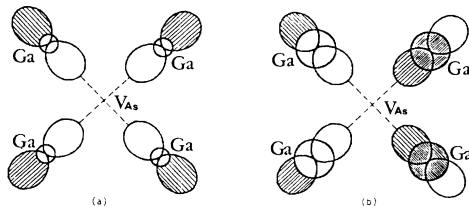


FIG. 5. Schematic representation of wave-function amplitudes for (a) the a_1 resonance at -0.25 eV and (b) the t_2 gap level at 1.29 eV for the neutral As vacancy in GaAs. The diameter of the s orbitals (circles) and the half-length of the p orbital (dumbbells) are scaled by their amplitudes. A hatched region in a wave function indicates a negative part of the wave function.

TABLE VII. Same as Table VI, but for the As vacancy in GaAs.

Charge state	a_1 (eV)	t_2 (eV)	t_2 - a_1 (eV)	t_2 level occupancy
V_{As}^{4-}	0.30	1.505	1.21	5
V_{As}^{3-}	0.19	1.468	1.28	4
V_{As}^{2-}	0.06	1.422	1.36	3
V_{As}^{1-}	-0.09	1.365	1.46	2
V_{As}^0	-0.25	1.295	1.55	1
V_{As}^{1+}	-0.41	1.210	1.62	0

levels are the same. In addition, the t_2 - a_1 splitting between the two upper levels for each vacancy has been opened up in our calculation compared to that in some other tight-binding calculations.^{9,19,20} We believe that this improvement is due to the inclusion of the off-diagonal perturbation around each vacancy as discussed by van der Rest *et al.*²¹

C. Predicted trends for the charged vacancies

We show in Fig. 6 our calculated energy levels in and near the fundamental gap for the ideal charged Ga and As vacancies in GaAs. The corresponding energy values of these levels are given in Tables VI and VII, together with some other information about the vacancies. For the t_2 symmetry, the levels corresponding to the charge states of the Ga vacancy are all located within the lower half of the fundamental gap and the levels corresponding

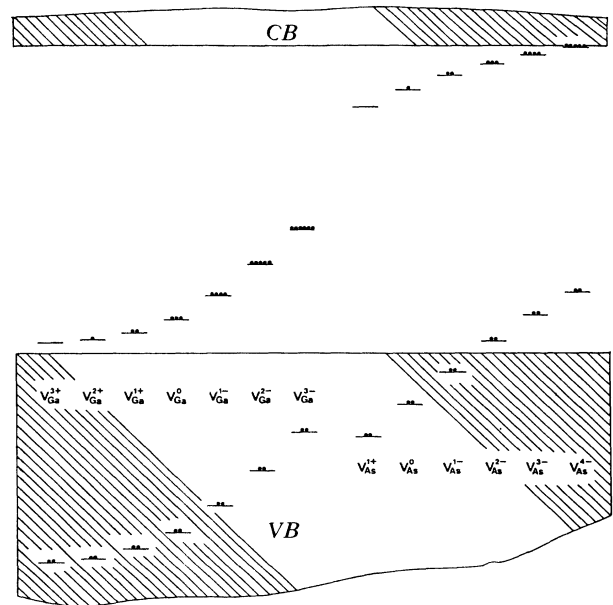


FIG. 6. Calculated defect-induced energy levels near the band gap for the undistorted neutral and charged vacancies in GaAs. VB and CB denote the valence band and conduction band, respectively. Solid circles indicate the occupancy of the defect levels. The upper level of each defect in this figure is t_2 symmetric, whereas the lower one is a_1 symmetric.

TABLE VIII. Calculated localization of the t_2 -symmetric gap levels on the orbitals of the atoms from the first- and second-nearest-neighbor shells of the Ga vacancy in GaAs. The energies of the levels are measured relative to the top of the valence band. $w^1 = 4w_s^1 + 12w_{p_x}^1$ is the level localization on the four nearest-neighbor atoms and $w^2 = 12w_s^2 + 12w_{p_x}^2 + 24w_{p_y}^2$ is the level localization on the 12 second-nearest-neighbor atoms. Note that $w_{p_z}^2$ is equal to $w_{p_y}^2$.

Charge state	Energy level (eV)	Level localization						
		w_s^1	$w_{p_x}^1$	w^1	w_s^2	$w_{p_x}^2$	$w_{p_y}^2$	w^2
V_{Ga}^{3-}	0.605	0.0135	0.0445	0.588	0.0036	0.0054	0.0028	0.174
V_{Ga}^{2-}	0.436	0.0118	0.0447	0.583	0.0029	0.0046	0.0028	0.157
V_{Ga}^{1-}	0.283	0.0099	0.0435	0.561	0.0022	0.0037	0.0028	0.138
V_{Ga}^0	0.168	0.0081	0.0402	0.515	0.0017	0.0029	0.0027	0.119
V_{Ga}^{1+}	0.100	0.0066	0.0357	0.455	0.0013	0.0022	0.0024	0.101
V_{Ga}^{2+}	0.068	0.0054	0.0311	0.395	0.0011	0.0018	0.0022	0.086
V_{Ga}^{3+}	0.051	0.0046	0.0271	0.344	0.0009	0.0015	0.0019	0.074

TABLE IX. Same as Table VIII, but for the As vacancy in GaAs.

Charge state	Energy level (eV)	Level localization						
		w_s^1	$w_{p_x}^1$	w^1	w_s^2	$w_{p_x}^2$	$w_{p_y}^2$	w^2
V_{As}^{4-}	1.505	0.0601	0.0071	0.326	0.0063	0.0092	0.0069	0.352
V_{As}^{3-}	1.468	0.0624	0.0080	0.346	0.0060	0.0091	0.0074	0.358
V_{As}^{2-}	1.422	0.0645	0.0091	0.367	0.0057	0.0089	0.0077	0.361
V_{As}^{1-}	1.365	0.0660	0.0104	0.389	0.0053	0.0087	0.0081	0.363
V_{As}^0	1.295	0.0670	0.0120	0.411	0.0049	0.0082	0.0084	0.359
V_{As}^{1+}	1.210	0.0671	0.0137	0.433	0.0044	0.0077	0.0087	0.353

TABLE X. Self-consistent spin-orbital occupation numbers n_α and atomic occupation numbers n for the neighbors of the Ga vacancy in GaAs. The superscripts 1 and 2 indicate the first- and second-nearest neighbor of the vacancy, respectively. Note that the occupation number $n_{p_z\sigma}^2$ is equal to $n_{p_y\sigma}^2$.

Defect	$n_{s\sigma}^1$	$n_{p_x\sigma}^1$	n^1	$n_{s\sigma}^2$	$n_{p_x\sigma}^2$	$n_{p_y\sigma}^2$	n^2
V_{Ga}^{3-}	0.911	0.569	5.237	0.668	0.258	0.242	2.822
V_{Ga}^{2-}	0.905	0.566	5.207	0.664	0.255	0.243	2.811
V_{Ga}^{1-}	0.902	0.562	5.178	0.661	0.253	0.243	2.802
V_{Ga}^0	0.901	0.558	5.153	0.660	0.252	0.242	2.796
V_{Ga}^{1+}	0.901	0.556	5.137	0.660	0.252	0.242	2.792
V_{Ga}^{2+}	0.902	0.554	5.127	0.659	0.252	0.242	2.790
V_{Ga}^{3+}	0.902	0.553	5.122	0.659	0.252	0.241	2.788

TABLE XI. Same as Table X, but for the As vacancy in GaAs.

Defect	$n_{s\sigma}^1$	$n_{p_x\sigma}^1$	n^1	$n_{s\sigma}^2$	$n_{p_x\sigma}^2$	$n_{p_y\sigma}^2$	n^2
V_{As}^{4-}	0.884	0.199	2.959	0.868	0.607	0.572	5.238
V_{As}^{3-}	0.851	0.205	2.935	0.864	0.602	0.575	5.231
V_{As}^{2-}	0.816	0.213	2.908	0.860	0.598	0.577	5.223
V_{As}^{1-}	0.778	0.221	2.879	0.857	0.594	0.578	5.214
V_{As}^0	0.737	0.227	2.847	0.855	0.592	0.578	5.204
V_{As}^{1+}	0.697	0.236	2.813	0.853	0.591	0.576	5.193

to the charge states of the As vacancy are located in the upper half of the gap. Here we have not shown the energy level for the most negatively charged As vacancy. The t_2 level in this case is located at an energy above, but very close to the conduction-band edge. As is supported by some other calculations,^{21,34} the Ga and the As vacancy have the charged t_2 levels either in the upper (As) or in the lower (Ga) half of the fundamental gap, in contrast to silicon where the ideal vacancy has a neutral t_2 level in the middle of the fundamental gap, and the charged t_2 levels can be located in both the lower and upper halves of the gap. Also, in the density-functional-theory calculation by Baraff and Schlüter,³⁵ four charge states for the Ga vacancy (V_{Ga}^0 , V_{Ga}^{1-} , V_{Ga}^{2-} , and V_{Ga}^{3-}) are found in the lower half of the band gap. For the As vacancy, however, these authors find only V_{As}^{1+} in the gap, in disagreement with Refs. 3, 21, 34, and the present work. Our calculation shows also that the t_2 - a_1 splittings are almost constant for the Ga vacancy but not quite so for the As vacancy in GaAs (see Tables VI and VII). If we look in more detail at Tables VI and VII, we find that for both the Ga and the As vacancy the t_2 - a_1 splittings become larger as the energies of the t_2 gap levels become lower.

The energy shift of the defect levels is not a linear function of the charge state of the vacancy. This is different from the results in the calculation by van der Rest *et al.*²¹ where an approximately linear function of the energy shift with the charge state was found. The non-linearity of the ionization energies with the charge state of a vacancy was also found in the self-consistent LMTO Green's-function calculation of Puska.³⁴ Furthermore, our result for the energy difference between two (charged) t_2 levels, whose occupancies differ by one electron, is in good agreement with the recent experimental work of Corbel *et al.*³ for the As vacancy. For example, they found two Fermi-level-controlled transitions: one is located at 0.035 eV and the other at 0.10 eV below the conduction band. They proposed that these two energies correspond to the two charge-state transitions $V_{\text{As}}^{2-} \rightarrow V_{\text{As}}^{-}$ and $V_{\text{As}}^{-} \rightarrow V_{\text{As}}^0$, respectively. In our calculation, we obtain $E_c - 0.088$ eV for V_{As}^{2-} and $E_c - 0.145$ eV for V_{As}^{-} , respectively. The energy difference between the two levels is 0.057 eV, which is comparable with the experimental finding, 0.065 eV, of Corbel *et al.*

The calculated localizations of the t_2 gap states for the Ga and As vacancies are listed in Tables VIII and IX, respectively. We first note that the t_2 gap state wave function for the Ga vacancy is more localized within the first shell of atoms than in the region of the second shell of atoms ($w^1 > w^2$), but that for the As vacancy the wave function is more evenly spread out ($w^1 \approx w^2$). Furthermore, in the region very close to the vacancies, the t_2 gap levels for the charge states of the Ga vacancy are mainly p -like, whereas the charge states of the As vacancy are largely s -like. These features are the same as that for the corresponding neutral vacancies. It would be expected that the t_2 gap states become less localized when their energies are close to the gap edges. For instance, for the t_2 gap state of V_{Ga}^{2+} at 0.068 eV above the top of the valence band, about 48.1% of the bound electrons reside in the

first- and the second-nearest-neighbor atoms of the vacancy, compared with about 76.2% for the t_2 gap state of V_{Ga}^{3-} at 0.605 eV. For the t_2 gap state of V_{As}^{4-} at 0.005 eV below the bottom of the conduction band, about 67.8% of the bound electrons are located in the perturbed region, compared with 77.0% for the t_2 gap state of V_{A}^0 at $E_c - 0.215$ eV.

Finally, the self-consistent spin-orbital occupation numbers n_α and the atomic occupation numbers n for the neighbors of the isolated Ga and As vacancies, where n is defined as the sum of the spin-orbital occupation numbers $\{n_\alpha\}$ on an atom, are listed in Tables X and XI. In the actual calculations, we first determined the atomic occupation numbers for one first- and one second-nearest-neighbor atoms of a neutral vacancy by the neutrality condition. The results are $5.153e^-$ and $2.796e^-$ for the neutral Ga vacancy and $2.847e^-$ and $5.204e^-$ for the neutral As vacancy. The net charge on one of the atoms close to a charged vacancy is then obtained by subtracting the occupation number of that atom when the vacancy is neutral from the occupation number when the vacancy is charged. In addition, the net charge in the region around a vacancy in a charge state can be calculated as the sum of the net charges in the first- and second-nearest-neighbor atoms to the vacancy. The results show that when we add one electron to the t_2 gap state of a vacancy, the net charge around the vacancy is changed by only a small amount, about 10% if we consider only the net charges on the four first-nearest-neighbor atoms and about 20% if we consider all the atoms up to the second-nearest neighbors of the vacancy. This is due to the effective charge screening in the crystal.

IV. SUMMARY

In this paper we have reported calculations on the electronic structure of undistorted neutral and charged Ga and As vacancies in GaAs. Some general features of the bound states for energies above the top of the valence band for the isolated vacancies in III-V compound semiconductors have been described by a simple model in terms of chemical bonds. We concluded that the bound state in the fundamental gap for a cation vacancy consists essentially of p orbitals centered on the nearest neighbors and that the bound state in the fundamental gap for an anion vacancy consists of both s and p orbitals of the nearest-neighboring atoms, of which one s orbital contributes more to the formation of the bound state than one p orbital. The detailed calculation for the neutral Ga and As vacancies supported this description for the electronic structure of the isolated vacancies in III-V compound semiconductors. In addition, our calculation revealed that the local electronic structure of the Ga vacancy is dominated by two localized a_1 states (at -9.65 and -0.88 eV) and two t_2 states (at -9.50 and 0.17 eV) and that the local electronic structure of the As vacancy is dominated by two localized a_1 states (at -6.86 and -0.25 eV) and one t_2 state (at 1.30 eV). The results agree well with the local-density calculation of Bachelet *et al.*¹³ The local electronic properties of these characteristic states can be understood very well in our simple

models based on the orbital interactions between cations and anions in the III-V compound semiconductors.

For the charge states of the vacancies we have found that the t_2 gap levels of the Ga vacancy are located in the lower half of the fundamental gap, whereas the corresponding levels for the As vacancy are in the upper half of the gap. The energy shifts of the defect levels as a function of the charge state of the vacancies are small, especially for the charged states of the As vacancy (smaller than 0.1 eV per bound electron in the t_2 state of the As vacancy). Comparison of our calculated energy values of the gap levels for the two negatively charged states of the As vacancy with the positron-annihilation-spectroscopy data of Corbel *et al.*³ for two Fermi-level-controlled transitions of the arsenic vacancy confirms the small charge-splitting effect. The local electronic features of the t_2 gap states in the charged vacancy are qualitatively the same as in the case of the neutral vacancies. Finally, we have shown that although the bound state in the gap is localized, the net charge in the region up to the second-nearest neighbors of the vacancy is changed by about 10–30 % of the bound electrons when adding electrons to the t_2 bound state, which means that the charge screening effect has been automatically accounted for in our calculation.

ACKNOWLEDGMENTS

One of us (H.X.) would like to thank Professor Lars Hedin for useful discussions and kind support. We are grateful to Dr. C. M. M. Nex at Cavendish Laboratories (Cambridge, United Kingdom) for supplying us with a version of the Cambridge Recursion Library.

APPENDIX

In the present paper, we described how to determine the weights of the localized states for given orbitals. The square roots of these weights give the absolute values of the projection (decomposition coefficients) of the wave function for the localized states on the basis orbitals. Much information (for example, local densities of states, level localizations, etc.) could be obtained from these calculated weights. In order to find the wave functions, however, we must know the relative signs of the absolute values of the projection coefficients. Note that since the Hamiltonian matrix is real, the decomposition coefficients can all be chosen real.

In principle, a symmetric localized states $|\psi^{(\nu)}\rangle$ with symmetry label ν can be expressed as a linear combination of a set of basis orbitals $\{|\phi_i^{(\nu)}(R)\rangle\}$ as follows:

$$|\psi^{(\nu)}\rangle = \sum_{i,R} c_i^{(\nu)}(R) |\phi_i^{(\nu)}(R)\rangle, \quad (\text{A1})$$

where $|\phi_i^{(\nu)}(R)\rangle$ is the i th ν -symmetric basis orbital constructed from the atomic orbitals centered on the atoms a distance R from the symmetry point, and $c_i^{(\nu)}(R)$ is the projection coefficient of the localized state $|\psi^{(\nu)}\rangle$ on the orbital $|\phi_i^{(\nu)}(R)\rangle$. Assuming orthogonality, the weights

of the localized state $|\psi^{(\nu)}\rangle$ on the basis orbital $|\phi_i^{(\nu)}(R)\rangle$ can be written as

$$w_i^{(\nu)}(R) = |c_i^{(\nu)}(R)|^2. \quad (\text{A2})$$

Thus, the coefficient $c_i^{(\nu)}(R)$ can only have one of the two values $\pm[w_i^{(\nu)}(R)]^{1/2}$.

To keep the notation even simpler, suppose the wave function $|\psi\rangle$ for the localized (gap) state can be written as [cf. (A1)]

$$|\psi\rangle = c_s |\phi_s\rangle + c_p |\phi_p\rangle + \dots, \quad (\text{A3})$$

where $|\phi_s\rangle$ ($|\phi_p\rangle$) denotes a symmetrized orbital constructed from s orbitals (p orbitals pointing towards the vacancy) on the four nearest neighbors of the vacancy (giving functions of either a_1 or t_2 symmetry in T_d). The terms not explicitly given in Eq. (A3) correspond to the symmetrized orbitals on the second, third, etc., shells of neighbors to the vacancy and to the symmetrized p orbitals perpendicular to $|\phi_p\rangle$ on the first shell.

After we have calculated the weights $w_s = |\langle \psi | \phi_s \rangle|^2$ and $w_p = |\langle \psi | \phi_p \rangle|^2$ with the recursion method, the expansion of $|\psi\rangle$ is either

$$|\psi^+\rangle = w_s^{1/2} |\phi_s\rangle + w_p^{1/2} |\phi_p\rangle + \dots \quad (\text{A4})$$

or

$$|\psi^-\rangle = w_s^{1/2} |\phi_s\rangle - w_p^{1/2} |\phi_p\rangle + \dots \quad (\text{A5})$$

In order to find out which of these combinations presents the correct linear combination, we define two test orbitals by simply normalizing the two terms in (A4) and (A5):

$$|\chi^+\rangle = \frac{w_s^{1/2} |\phi_s\rangle + w_p^{1/2} |\phi_p\rangle}{(w_s + w_p)^{1/2}}, \quad (\text{A6})$$

$$|\chi^-\rangle = \frac{w_s^{1/2} |\phi_s\rangle - w_p^{1/2} |\phi_p\rangle}{(w_s + w_p)^{1/2}}. \quad (\text{A7})$$

We then obtain the following relations:

$$\begin{aligned} \langle \psi^+ | \chi^- \rangle &= \langle \psi^- | \chi^+ \rangle \\ &= \frac{w_s - w_p}{(w_s + w_p)^{1/2}} \leq \frac{w_s + w_p}{(w_s + w_p)^{1/2}} \\ &= \langle \psi^+ | \chi^+ \rangle = \langle \psi^- | \chi^- \rangle. \end{aligned} \quad (\text{A8})$$

If we first suppose that $|\psi^+\rangle$ is the correct linear combination $|\psi\rangle$, we see that $|\psi\rangle$ has a larger projection on $|\chi^+\rangle$ than on $|\chi^-\rangle$. Furthermore, if we assume that $|\psi^-\rangle$ is the correct linear combination $|\psi\rangle$, we see that it has a larger projection on $|\chi^-\rangle$ than on $|\chi^+\rangle$. This means that if we use the recursion method to calculate the projection weights $|\langle \psi | \chi^+ \rangle|^2$ and $|\langle \psi | \chi^- \rangle|^2$, we can decide if $|\psi\rangle$ is best represented by $|\psi^+\rangle$ or by $|\psi^-\rangle$: if $|\langle \psi | \chi^+ \rangle|^2 > |\langle \psi | \chi^- \rangle|^2$, then $|\psi^+\rangle$ is the correct linear combination, whereas if $|\langle \psi | \chi^+ \rangle|^2 < |\langle \psi | \chi^- \rangle|^2$, then $|\psi^-\rangle$ is the correct linear combination.

- ¹*Deep Centers in Semiconductors: A State of the Art Approach*, edited by S. T. Pantelides (Gordon and Breach, New York, 1986).
- ²D. V. Lang, in *Radiation Effects in Semiconductors, 1976*, IOP Conf. Ser. No. 31, edited by N. B. Urli and J. W. Corbett (IOP, Bristol, 1977), p. 70.
- ³C. Corbel, M. Stucky, P. Hautojärvi, K. Saarinen, and P. Moser, *Phys. Rev. B* **38**, 8912 (1988).
- ⁴T. A. Kennedy and N. D. Wilsey, *Phys. Rev. Lett.* **41**, 977 (1978); *Phys. Rev. B* **23**, 6585 (1981).
- ⁵T. A. Kennedy, N. D. Wilsey, J. J. Krebs, and G. H. Stauss, *Phys. Rev. Lett.* **50**, 1281 (1983).
- ⁶J. C. Bourgoin, H. J. von Bardeleben, and D. Stievenard, *Phys. Status Solidi A* **102**, 499 (1987).
- ⁷S. Dannefaer, *J. Phys. C* **15**, 599 (1982); S. Dannefaer, B. Hogg, and D. Kerr, *Phys. Rev. B* **30**, 3355 (1984).
- ⁸G. Dlubek, O. Brümmer, F. Plazaola, and P. Hautojärvi, *J. Phys. C* **19**, 331 (1986); G. Dlubek and R. Krause, *Phys. Status Solidi A* **102**, 443 (1987).
- ⁹J. Bernholc and S. T. Pantelides, *Phys. Rev. B* **18**, 1780 (1978).
- ¹⁰G. A. Baraff and M. Schlüter, *Phys. Rev. Lett.* **41**, 892 (1978); *Phys. Rev. B* **19**, 4965 (1979).
- ¹¹J. Bernholc, N. O. Lipari, and S. T. Pantelides, *Phys. Rev. Lett.* **41**, 895 (1978); *Phys. Rev. B* **21**, 3545 (1980).
- ¹²U. Lindefelt and A. Zunger, *Phys. Rev. B* **26**, 846 (1982).
- ¹³G. B. Bachelet, G. A. Baraff, and M. Schlüter, *Phys. Rev. B* **24**, 915 (1981).
- ¹⁴R. Strehlow, M. Hanke, and W. Kühn, *Phys. Status Solidi B* **131**, 631 (1985).
- ¹⁵J. R. Chelikowsky and M. L. Cohen, *Phys. Rev. B* **14**, 556 (1976).
- ¹⁶U. Lindefelt, *J. Phys. C* **11**, 3651 (1978).
- ¹⁷C. W. Myles and O. F. Sankey, *Phys. Rev. B* **29**, 6810 (1984).
- ¹⁸D. N. Talwar and C. S. Ting, *J. Phys. C* **15**, 6573 (1982).
- ¹⁹D. N. Talwar and C. S. Ting, *Phys. Rev. B* **25**, 2660 (1982).
- ²⁰S. D. Sarma and A. Madhukar, *Phys. Rev. B* **24**, 2051 (1981).
- ²¹J. van der Rest and P. Pecher, *J. Phys. C* **17**, 85 (1984).
- ²²J. C. Slater and G. F. Koster, *Phys. Rev.* **94**, 1498 (1954).
- ²³M. Wolfsberg and L. Helmoltz, *J. Chem. Phys.* **20**, 837 (1952).
- ²⁴W. A. Harrison, *Phys. Rev. B* **23**, 5230 (1981).
- ²⁵P. Pecher, E. Kauffer, and M. Gerl, in *Defects and Radiation Effects in Semiconductors, 1978*, IOP Conf. Proc. Ser. No. 46, edited by J. H. Albany (IOP, London, 1979), p. 174; P. Pecher, G. Toussaint, and M. Lannoo, in *Defects and Radiation Effects in Semiconductors, 1980*, IOP Conf. Proc. Ser. No. 59, edited by R. R. Hasiguti (IOP, London, 1981), p. 147.
- ²⁶O. F. Sankey and J. D. Dow, *Phys. Rev. B* **27**, 7641 (1983).
- ²⁷S. Lee and J. D. Dow, *Phys. Rev. B* **31**, 3910 (1985).
- ²⁸R. Haydock, in *Solid State Physics*, edited by H. Ehrenreich, F. Seitz, and D. Turnbull (Academic, New York, 1980), Vol. 35, p. 215.
- ²⁹R. Haydock, V. Heine, and M. J. Kelly, *J. Phys. C* **5**, 2845 (1972).
- ³⁰C. M. M. Nex, in *The Recursion Method and Its Applications*, Vol. 58 of *Springer Series in Solid-State Sciences*, edited by D. G. Pettifor and D. L. Weaire (Springer-Verlag, Berlin, 1985), p. 52.
- ³¹C. M. M. Nex, *J. Phys. A* **11**, 653 (1978).
- ³²B. N. Parlett, in *The Symmetric Eigenvalue Problem* (Prentice-Hall, Englewood Cliffs, NJ, 1980).
- ³³R. Haydock, in Ref. 30, p. 8.
- ³⁴M. J. Puska, *Phys. Status Solidi A* **102**, 11 (1987).
- ³⁵G. A. Baraff and M. Schlüter, *Phys. Rev. Lett.* **55**, 1327 (1985).